Effects of Non-Fixed Scatterers' Random Movements on Ultra-Wideband MISO Channels

Ana-Maria Pistea[*]

Abstract—Most wireless channel models assume fixed scatterers with specific geometrical distributions in the propagation environment. In reality most scatterers move with random movements on the azimuth plane. In this paper, the effects of such scatterers' random movements on the cross-correlation function (CCF) of wideband (WB) and ultra-wideband (UWB) non-isotropic multiple-input multiple-output (MIMO) channels are characterized. The CCF of WB/UWB MIMO channels is calculated not by assuming a specific geometry for scatterers in space but based on specific mathematical relationships between physical parameters of the wireless channel along with appropriate assumptions on their probability density functions (pdfs). The CCF is used to determine the influence of moving scatterers, in a stationary scenario, on the power spectral density (PSD) and the coherence time of WB and UWB multiple-input single-output (MISO) channels, as a particular case of MIMO channels. Unlike the fixed scatterers case, the PSD is not a band-limited process, it decays with frequency.

1. INTRODUCTION

Most propagation models assume that the scatterers are immobile or have a specific geometrical distribution on the azimuth plane. In reality only some of these scatterers are fixed, most of them move in a non-systematic manner while their displacement rarely has a geometric shape.

Since the influence of random displacements of scatterers on wideband (WB) and ultra-wideband (UWB) multiple-input multiple-output (MIMO) non-isotropic outdoor wireless channels has not been studied in a closed-form in literature, the contribution of this paper consists in developing a model which realistically predicts the impact of moving scatterers on these types of channels [1–3]. This topic is of great concern since UWB technology in combination with MIMO systems finds more and more applications in areas such as location tracking for outdoor emergency services [4, 5], location tracking and sensor for mobile outdoor users [6], medical [7] and electronic warfare applications [3]. Moreover, some research results [8–10] proved that a joint radar and wireless communication system would constitute a unique platform for future intelligent environmental sensing and ad-hoc communication networks, in terms of both spectrum efficiency and cost effectiveness. This evolution regarding the use of UWB systems in outdoor environments as radar or communication systems has led to the formulation of specific requirements aimed at investigating the influence of outdoor propagation on UWB mobile systems [11].

The proposed model is an extension of the work presented in [12] where the scatterers were considered to be fixed. The impact of moving scatterers is analyzed by determining the statistical behavior of the space-time-frequency channel transfer function which is used to calculate the cross-correlation function (CCF) between two sub-channels of a mobile multicarrier MIMO channel. The Fourier analysis of the CCF is used to determine the influence of moving scatterers on the power

* Corresponding author: Ana-Maria Pistea (ampistea@gmail.com).

The author is with the Department of Communications and Military Electronic Systems, Military Technical Academy, Bucharest, Romania.

spectral density (PSD) of multiple-input single-output (MISO) channels as a particular case of MIMO channels. The CCF is also used to determine the coherence time for both WB and UWB MISO channels.

The rest of the paper is organized as follows: notations and assumptions are introduced in Section 2. The effects of scatterers' displacements on the CCF are examined in Section 3. The proposed CCF is used to analyze the PSD and the coherence time in Section 4. Conclusions are summarized in Section 5.

2. NON-ISOTROPIC SCATTERING ENVIRONMENT WITH MOVING SCATTERERS

The propagation environment that underlies the derivation of the channel transfer function and CCF with random movements of scatterers is illustrated in Figure 1 where a pair of base station — mobile station antennas of a MIMO system is displaced in a two-dimensional (2D) non-isotropic propagation environment. The variations of WB and UWB channels parameters with frequency and the tendency of the multipath waveforms, i, to group into clusters, l, are also considered.
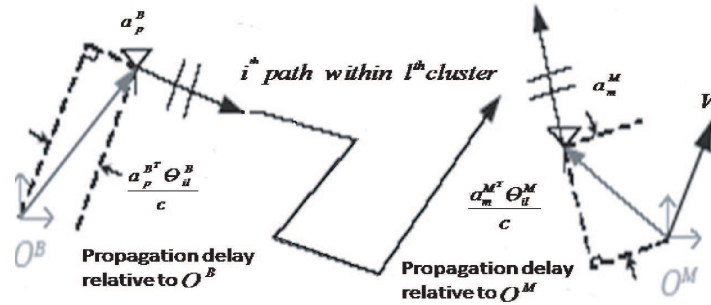
Figure 1. Moving MS on the azimuth plane with constant speed vector V; pth and mth antennas of the BS and MS located at a_p^B and at a_m^M in their local coordinates, O^B and O^M.

Scatterers' motion is Brownian (random) based on stationary-increment Wiener process, while the mobile station moves with constant speed on the azimuth plane. The mobile station and base station receive a large number of waveforms reflected from moving scatterers. The movements of each scatterer change the relative distance of the scatterer to the mobile station coordinate. Therefore, it has a direct effect on the propagation delay caused by that scatterer. While the mobile station moves with a constant speed on the azimuth plane, it may have other movements like arbitrary rotations around the azimuth axis. In this situation, almost all rotational movements of the mobile station are to align the coordinate with the direction of its trajectory. These rotations are usually very slowly varying with time and with low impacts on the CCF, therefore are ignored in this paper [13].

Scatterers' distribution in space does not have a specific geometry: in contrast to most MIMO-CCF models that employ a certain geometry for scatterers around the mobile station, the proposed model is based on mathematical relationships among channel gain, time-delay and pathloss exponent, rather than the scatterers' geometry. These relationships substitute the role of the scatterers' geometry to represent the power of the multipath components. Such an approach enables the model to consider different propagation environments along with different antenna patterns in the CCF expression.

Assumptions A1)–A4) illustrate how the above mentioned properties are integrated into the model:

A1) Base station antennas array are fixed. The displacement of the mobile station is represented by a 2D constant vector, V. The displacements of the $i \times l$th scatterer, $X_{il}^s(t) \triangleq \begin{bmatrix} x_{il,1}^s(t) \\ x_{il,2}^s(t) \end{bmatrix}$, follow a 2D stationary-increment Wiener random vector [14, Chapter 10]. The two components of $X_{il}^s(t)$, $x_{il,1}^s(t)$ and $x_{il,2}^s(t)$, are independent non-stationary zero-mean Normal random processes with stationary-independent increments [14].

A2) The complex antenna propagation patterns (APPs), $G_p^B(\Theta_{il}^B, \omega)$ and $G_m^M(\Theta_{il}^M, \omega)$, of the pth antenna at the base station and the mth antenna at the mobile station give the response of the pattern

elements in terms of the propagation directions and the central frequency, ω. Antenna elements are located around the mobile station and the base station local coordinates, O^M and O^B, with relative position vectors a_p^B and a_m^M, respectively. These are periodic functions with period 2π. Therefore, are represented by their Fourier series expansions (see [12, 13] for the Fourier series expansions of some APPs):

$$G\left(\Theta;\omega\right) = \sum_{k=-\infty}^{\infty} \mathcal{G}_k e^{jk\Theta}, \quad \mathcal{G}_k = \frac{\displaystyle\int_{-\pi}^{\pi} G\left(\Theta;\omega\right)}{2\pi} e^{-jk\Theta} d\Theta \tag{1}$$

A3) The pdf of the propagation directions, known as azimuth angle spreads, $f^B(\Theta^B)$ and $f^M(\Theta^M)$, for the range $[-\pi,\pi)$ characterizes the non-isotropic propagation channel. These pdfs are periodic functions with period 2π and can be represented by their Fourier series expansions as follows.

$$f_\Theta\left(\Theta\right) = \sum_{k=-\infty}^{+\infty} \mathcal{F}_k e^{jk\Theta}, \quad \mathcal{F}_k = \frac{\displaystyle\int_{-\pi}^{\pi} f_\Theta\left(\Theta\right) e^{-jk\Theta} d\Theta}{2\pi} \tag{2}$$

Reported measurement results suggest Laplace and von-Mises pdfs for WB and UWB propagation channels [12]. Since these pdfs are periodic functions with period 2π, in Table 1 are represented by the corresponding Fourier series expansions:

Table 1. Non-isotropic azimuth angle spread and corresponding Fourier series expansions.

PDF, $f_\Theta\left(\Theta\right)$, $\forall \Theta \in [-\pi, \pi)$, $\mathcal{F}_k$	
Laplace	$f_\Theta\left(\Theta\right) = \dfrac{e^{\left\vert\frac{-\sqrt{2}\Theta}{\sigma}\right\vert}}{\sqrt{2}\sigma}$
	$\mathcal{F}_k = \dfrac{e^{-\frac{\pi\left(\sqrt{2}+jk\sigma\right)}{\sigma}}\left(e^{\frac{2\sqrt{2}\pi}{\sigma}}-e^{j2k\pi}\right)}{2\pi\left(j\sqrt{2}k\sigma-2\right)}$
von-Mises	$f_\Theta\left(\Theta\right) = \dfrac{e^{\vert n*cos(\Theta-\mu)\vert}}{2\pi J_0(n)}$
	$\mathcal{F}_k = \dfrac{J_k(n)}{J_0(n)}$

Von-Mises pdf is strongly influenced by parameter n which determines the order of the channel non-isotropy. In other words, n controls the width of direction of arrival (DOA) of scattered components, and n can take values in the range $n \in [0,\infty)$. When $n \to \infty$, $f_{\Theta^M}(\Theta) = \delta(\Theta - \mu)$, the propagation environment is considered extremely-nonisotropic-scattered centrated at $\Theta = \mu$, where $\mu \in [-\pi, \pi)$ is the mean DOA at the mobile station. For large n, say $3 \leq n \leq 20$, a typical non-isotropic environment can be considered. When Fourier series coefficients are determined, parameter n appears in the argument of the Bessel functions represented by the modified Bessel function of the first kind, $J_k(\cdot)$, and the zero-order modified Bessel function, $J_0(\cdot)$. The isotropic propagation environment can be mathematically represented in a similar way, using the following expression of the Fourier series expansions: $\mathcal{F}_k = \frac{1}{2\pi}\delta_k$.

A4) The propagation delay over the ith path within lth cluster is time-varying. This is the consequence of both linear speed of the mobile station and random displacements of the $i \times l$th scatterer from its initial position. This consequence appears when the random movement of each scatterer changes the relative distance of the scatterer to the mobile station coordinate. Therefore, it has a direct effect on the propagation delay caused by that scatterer. In these circumstances, the time-varying propagation delay over the ith path within the lth cluster is given by:

$$\tau_{pm,il}\left(t\right) \triangleq \tau_{pm,il}\left(0\right) + \frac{1}{c}\left(X_{il}^S\left(t\right) + Vt\right)^T \Theta_{il}^M \tag{3}$$

where $(\cdot)^T$ is the transpose operator and c the speed of light. At time zero, the propagation delay of the ith path within the lth cluster, $\tau_{pm,il}(0)$, is decomposed into three components: one major propagation delay and two relative propagation delays with respect to the base station and the mobile station local coordinates, O^B and O^M, as follows: $\tau_{pm,il}(0) = \tau_{il} - (\tau_{p,il}^B + \tau_{m,il}^M)$, where $\tau_{p,il}^B \triangleq \frac{a_p^B \Theta_{il}^B}{c}$ and $\tau_{m,il}^M \triangleq \frac{a_m^M \Theta_{il}^M}{c}$. The term τ_{il} represents the propagation delay between O^B and O^M, $\tau_{p,il}^B$ and $\tau_{m,il}^M$ are the relative propagation delays from antennas, a_p^B, a_m^M.

Based on the above mentioned properties of scatterers and using Assumptions A1)–A4), the channel transfer function expression with moving scatterers influence is given by:

$$h_{pm}(t,\omega) = \left(\frac{\omega_{bw}}{\omega}\right)^\eta \sum_{l=1}^{L}\sum_{i=1}^{I} G_p^B\left(\Theta_{il}^B,\omega\right) G_m^M\left(\Theta_{il}^M,\omega\right) \times g_{pm,il} e^{j\left(\phi_{il} - \frac{\omega}{c}\left(X_{il}^S(t)+Vt\right)^T \Theta_{il}^M - \omega T_{pm,l} - \omega \tau_{pm,il}(t)\right)} \quad (4)$$

In Equation (4), the channel transfer function is represented by a sum of propagation waveforms over a number of i paths and l clusters (with maximum I paths and L clusters). Each i path within each l cluster is associated with the following parameters: direction of departure (DOD) — Θ_{il}^B from the base station and DOA — Θ_{il}^M to the mobile station, complex gain of WB and UWB APPs — $G(\Theta_{il},\omega)$, time-varying delay, $\tau_{pm,il}(t)$, of the ith path within lth cluster and fixed cluster delay, $T_{pm,l}$, path phase shift, ϕ_{il}, frequency dependent path gain, $g_{pm,il} = \frac{1}{2\omega\tau_{il}}$.

The channel frequency selectivity is considered by introducing, for both WB and UWB channels, the term $(\frac{\omega_{bw}}{\omega})^\eta$, where ω was previously defined, and ω_{bw} is the channel bandwidth and η the path-loss exponent [12]. In the case of UWB channel, this term is not enough to have a realistic representation of the frequency selectivity phenomenon since UWB APP is frequency selective while WB APP is not. Thus, two approaches for 2D APP calculation are used: for WB signals, APP is calculated depending on the central angular frequency while for UWB channels, APP is calculated depending on the central frequency and by integrating $G(\Theta_{il},\omega)$ across all the frequencies of the transmitted signal.

Based on the previous assumptions, the space-time-frequency CCF between the channel transfer functions of two arbitrary MIMO communication links $h_{pm}(t_1,\omega_1)$ and $h_{qn}(t_2,\omega_2)$ is derived using the following equation:

$$R_{pm,qn}(t_1,t_2,\omega_1,\omega_2) \triangleq E\left[h_{pm}(t_1,\omega_1) h_{qn}^*(t_2,\omega_2)\right] \quad (5)$$

After some mathematical manipulations the expression of $R_{pm,qn}(t_1,t_2,\omega_1,\omega_2)$ is decomposed as it is presented in Equation (6), where $F_{sel} = \frac{(\omega_{bw1}\omega_{bw2})^\eta}{(\omega_1\omega_2)^\eta(4\omega_1\omega_2)}$. The calculation methodology for the first three expectations in Equation (6) is the same as the one presented in [12] since they have the same expression as in the fixed scatterer case.

$$R_{pm,qn}(t_1,t_2;\omega_1,\omega_2) = F_{sel}\sum_{l=1}^{L}\sum_{i=1}^{I}\left\{E\left[(\tau_{i_2 l_2}\tau_{i_1 l_1})^{-1} e^{j\left((\omega_2\tau_{i_2 l_2}-\omega_1\tau_{i_1 l_1})+(\omega_1 T_{pm,l_1}-\omega_2 T_{qn,l_2})\right)}\right]\right.$$

$$\times E\left[e^{j\left(\phi_{i_1 l_1}-\phi_{i_2 l_2}\right)}\right]\Big\} E\left[G_p^B\left(\Theta_{i_1 l_1}^B;\omega_1\right) G_q^{B*}\left(\Theta_{i_2 l_2}^B;\omega_2\right) e^{j\left(\frac{\omega_1}{c}a_p^{B^T}\Theta_{i_1 l_1}^B - \frac{\omega_2}{c}a_q^{B^T}\Theta_{i_2 l_2}^B\right)}\right]$$

$$\times E\left[G_m^M\left(\Theta_{i_1 l_1}^M;\omega_1\right) G_n^{M*}\left(\Theta_{i_2 l_2}^M;\omega_2\right) e^{j\left(\frac{\omega_1}{c}\left(-X_{il}^S(t_1)-Vt_1+a_m^M\right)^T\Theta_{i_1 l_1}^M\right)} e^{j\left(\frac{\omega_2}{c}\left(X_{il}^S(t_2)+Vt_2-a_n^M\right)^T\Theta_{i_2 l_2}^M\right)}\right] \quad (6)$$

In order to calculate the last expectation in (6), first the calculation is performed on a simplified version of this expectation and for an arbitrary Wiener displacement process vector $X(t)$, as follows:

$$E\left[e^{\frac{j}{c}(\omega_2 X(t_2)-\omega_1 X(t_1)+d)\Theta_{il}^M}\right] = E\left[E_X\left[e^{\frac{j}{c}(\omega_2 X(t_2)-\omega_1 X(t_1))^T\Theta_{il}^M}\right] e^{\frac{j}{c}d^T\Theta_{il}^M}\right] \quad (7)$$

$E_X[\cdot]$ denotes the expectation with respect to the pdf of X, $E[\cdot]$ the expectation with respect to the pdf of all remaining random variables, and d an arbitrary 2D vector.

The frequency shift of the $i \times l$th received multipath waveform is caused by both random displacements of the $i \times l$th scatterer, $X_{il}^S(t)$, and the mobile station movements, i.e., Vt. After some

manipulations and using the results in [12], the expectations in (6) are calculated, and the CCF can be formulated as follows:

$$R_{pm,qn}(t_1, t_2; \omega_1, \omega_2) = F_{sel}\Phi_\tau^{(-1)}(j(\omega_1 - \omega_2)) \times \Phi_T(j(\omega_2 - \omega_1))$$

$$\times \left(\sum_{l=1}^{L}\sum_{i=1}^{I} e^{-\zeta_{i_1 l_1} t_1 \frac{\omega_1^2}{2c^2}} e^{\zeta_{i_2 l_2} t_2 \frac{\omega_2^2}{2c^2}}\right) \times \mathcal{W}\left(d_{pq}^B, \mathcal{H}_{k_{1,2}}^B\right) \times \mathcal{W}\left(d_{mn}^M, \mathcal{H}_{k_{1,2}}^M\right) \quad (8)$$

The elements denoted by $\Phi_{\tau,T}(s)$ represent the moment generating functions (MGFs) of the delay profile (τ, T) evaluated at the difference between two frequencies. The definition of the MGF of a random variable x with the PDF $f_X(x)$ is defined as follows: $\Phi_X(s) = E[e^{jsX}] = \int_{-\infty}^{\infty} e^{js\xi} f_X(\xi)d\xi$. The probability densities of the absolute times of arrival of clusters and paths used to calculate the MGFs are represented by:

$$p_{T_l}(T) = \frac{\Lambda^{L+1}T^L e^{-\Lambda T}}{L!}, \quad p_{\tau_{i,l}}(\tau) = \frac{\lambda^I \tau^{I-1} e^{-\lambda \tau}}{(I-1)!} \quad (9)$$

where Λ and λ are the cluster arrival rate and ray arrival rate. The parameter $\frac{1}{\Lambda}$ is typically in the range 10–50 ns, while $\frac{1}{\lambda}$ shows a wide variation from 0.5 ns in non line-of-sight (NLOS) situations, to more than 5 ns in LOS situations [2]. $\mathcal{W}(d, \mathcal{H}_k) \triangleq 2\pi \sum_{k=-\infty}^{\infty} j^k e^{jk\angle d}\mathcal{H}_k(\omega)J_k(\frac{|d|}{c})$ and $\mathcal{H}_k \triangleq \mathcal{G}_{p,k}(\omega) \otimes \mathcal{G}_{q,-k}^*(\omega) \otimes \mathcal{F}_k$.

The norm of the vectors, d_{pq}^B, d_{mn}^M, indicates the distance between antennas and shows the shifted distances between $\omega_1 a_p^B$ and $\omega_2 a_q^B$ at the base station, and between $\omega_1(a_m^M - t_1 V)$ and $\omega_2(a_n^M - t_2 V)$ at the mobile station, respectively. Parameters $d_{(\cdot)}^{(\cdot)}$ contain space, time, and frequency separations between $h_{pm}(t_1, \omega_1)$ and $h_{qn}(t_2, \omega_2)$. As it is seen in (8), the contribution of each moving scatterer is represented by its corresponding variance factor, ζ_{il}. A larger value of the variance factor indicates a faster decay of the $i \times l$th associated term in the CCF expression. It implies that scatterers with larger displacements have less effect on the CCF, while the effect of slow moving scatterers lasts longer.

3. NUMERICAL EVALUATION OF THE CCF

In this section, the CCF expression is used to examine the scatterers' random displacement influence on the PSD and on the coherence time, for $I = 10$, $L = 4$ and $\zeta = 0.008$. The propagation environment is non-isotropic (represented by two distributions of azimuth angle spread (Laplace and von-Mises)) and omnidirectional antennas are employed at the mobile station. When $\zeta \to 0$, the scatterers are fixed. As $\zeta \to \infty$ the correlation goes to zero regardless the antenna type or the distribution of the propagation environment.

This extensive simulation for different propagation environments as well as the mobile station speed covers basically all aspects of this modeling and all related parameters. For both PSD and coherence time evaluation, the presented results correspond to: WB channel — $f_c = 2.5$ GHz, $\omega_{bw} = 200$ MHz, UWB channel — $fc = 6.8$ GHz, $\omega_{bw} = 10.5$ GHz.

3.1. Effects of Scatterers' Random Displacements on the PSD

In order to investigate how the scatterers' random movements affect the PSD, $\omega_1 = \omega_2$ and $m = n = 1$, which transforms the MIMO channel in a multiple-input single-output (MISO) channel, is considered the stationary case. Considering $\angle d_{1,1}^M = \angle V + (1 - \angle(t_2 - t_1))\frac{\pi}{2}$ (in Radian) results the Fourier transform of the CCF versus the time-difference index $\Delta t \triangleq t_2 - t_1$:

$$R_{p1,q1}(\Lambda, \omega) \triangleq \int_{-\infty}^{\infty} e^{-j\Lambda\Delta t} R_{p1,q1}(t_1, t_2, \omega, \omega) d\Delta t$$

$$= 2\pi F_{sel}^2 \times \left\{\sum_{k=1}^{\infty} j^k e^{jk\angle V}\left(\mathcal{G}_{1,k}^M(\omega) \otimes \mathcal{G}_{1,-k}^{M*}(\omega) \otimes \mathcal{F}_k^M\right) \times \mathcal{W}\left(d_{p,q}^B, \mathcal{H}_k^B\right) \times \sum_{l=1}^{L}\sum_{i=1}^{I} C_k \frac{1}{j\Lambda + \frac{\zeta_{il}\omega^2}{2c^2}}\right\} (10)$$

Λ is a frequency variable in the interval $-\frac{\omega|V|}{c} < \Lambda \leq \frac{\omega|V|}{c}$, $C_k = \frac{T_k(\frac{c\Lambda}{|V|\omega})}{\sqrt{1-(\frac{c\Lambda}{|V|\omega})^2}}$, and the parameter

$T_k(\cdot) \triangleq \cos[k\cos^{-1}(\Lambda)]$ represents the Chebyshev polynomials which form a complete orthogonal set on the interval $-1 \leqslant u < 1$, with respect to the weighting function $\frac{1}{\sqrt{1-u^2}}$. The term $J_k(u) \triangleq \frac{j^{-k}}{\pi} \int_0^\pi e^{j(k\xi+u\cos\xi)}d\xi$ is the kth-order Bessel function. Using (10) and Fourier transform of $J_k(u)$, the Fourier transform of the CCF versus Δt results in:

$$R_\zeta^M(\Lambda) \triangleq \sum_{k_{1,2}=-\infty}^{\infty} \mathcal{H}_{1,k_{1,2}}^M e^{jk_1 \angle V} C_k \sum_{l=1}^{L} \sum_{i=1}^{I} \frac{1}{j\Lambda + \frac{\zeta_{il}\omega^2}{2c^2}} \tag{11}$$

Equation (11) represents the PSD, $R_\zeta^M(\Lambda)$, for the 2D propagation environment, which reflects the channel variations caused by the mobile station and the dispersion of the signal energy caused by the moving scatterers.

Figures 2 and 3 show the PSD of WB and UWB MISO channels for rectangular (omnidirectional) antenna in an environment with moving scatterers.
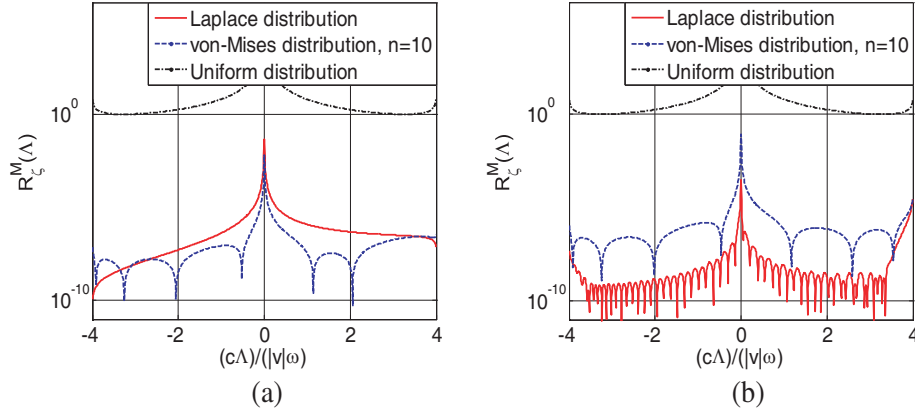
Figure 2. Moving scatterers influence on the PSD of (b) WB and (a) UWB channels, the mobile station moves on the positive direction of the x-axis.
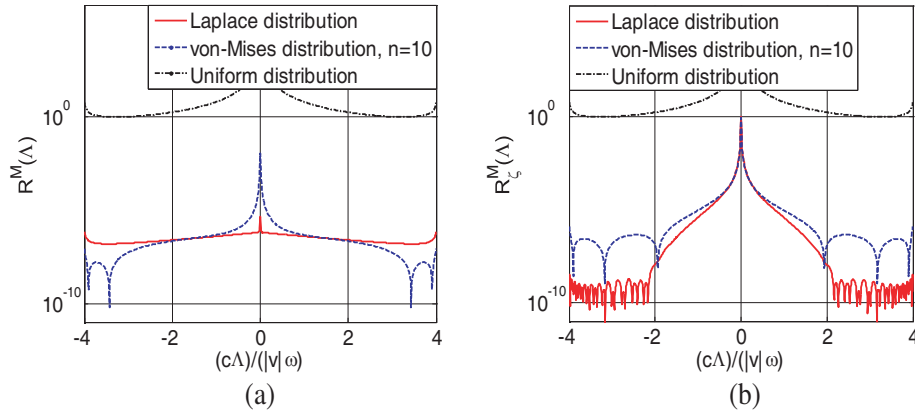
Figure 3. Moving scatterers influence on the PSD of (b) WB and (a) UWB channels, the mobile station moves on the positive direction of the y-axis.

The mobile station is moving in the positive direction of x-axis or y-axis. The PSD shape is asymmetrical or symmetrical as a consequence of the interaction among the beam of the APP, the direction of the mobile station speed and the distribution of the propagation directions around the

mobile station. It can be observed that the mobile station movement in the positive direction of the x-axis produces a PSD with larger values at positive Λ than at negative Λ. This asymmetry of the PSD is also determined by the Doppler spectrum which concentrates towards positive frequency axis. It can be observed how the energy is concentrated in the positive part of the x-axis giving rise to peaky spectra when $\Lambda = 0$. This is because of the random scatterers displacements which produce more pronounced waves scattering and hence increased angular spreads. Also, it is clearly observed that the movement of scatterers has a great impact on the channel PSD causing the PSD to be a non-bandlimited process, in contrast to the case when scatterers are fixed [12]. The envelope fluctuation of the PSD is significantly influenced by the antenna bandwidth, hence WB channels have a less fluctuating PSD than UWB channels because of the frequency selectivity which increases with signal frequency and bandwidth.

3.2. Effects of Scatterers' Random Displacements on the Coherence Time

Using CCF expression, the coherence time is determined with the following equation: $D_{\Delta t, \Delta \omega} \triangleq \frac{|R(t_1, t_2; \omega_1, \omega_2)|^2}{|R(t_1, t_1; \omega_1, \omega_1)|^2} = 0.5$, where $\Delta \omega = \omega_2 - \omega_1 \geqslant 0$, $\Delta t = t_2 - t_1 \geqslant 0$ and $coherence\,time = D_{\Delta t, 0}$. When the mobile station moves in any direction in space, the averaged coherence time over these directions is given by: $\overline{coherence\,time} \triangleq \frac{1}{2\pi} \int_{-\pi}^{\pi} coherence\,time\,(\angle V)\,d\,(\angle V)$.

Figures 4(a), (b) show the influences of both fixed and moving scatterers on the averaged coherence time depending on the mobile station speed and different distributions of the environment (Laplace, von-Mises).
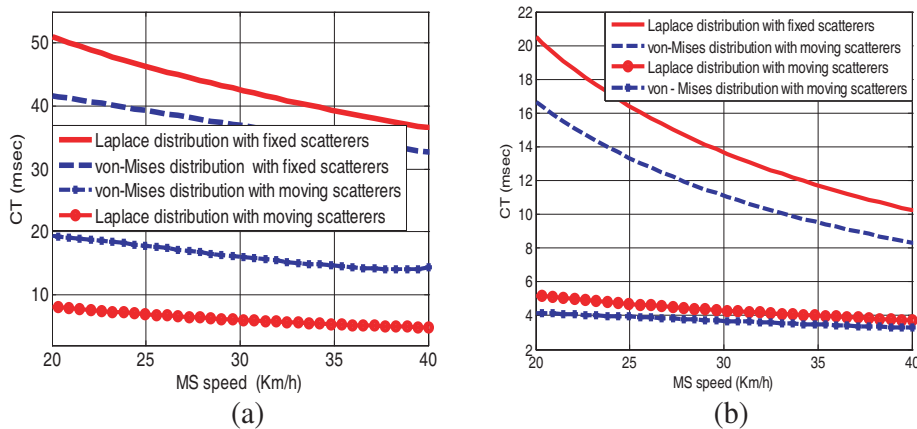
Figure 4. Average coherence tine of (a) WB and (b) UWB channels depending on the mobile station speed values, $|V|$, considering Laplacian and von-Mises pdfs.

In the mentioned figures the coherence time is designated as CT, and the mobile station is designated as MS for the sake of brevity. In the literature the coherence time is reported to be mostly a function of the mobile station speed [15]. This numerical investigation also confirms such a claim; however, it is also observed that the coherence time is influenced by other parameters. This result is expected based on the Fourier analysis of stationary CCF, since the Doppler effect appears as a function of the non-isotropic environment, the employed antenna at the mobile station and the mobile station speed direction. If the mobile station has a linear speed, the coherence time is usually reported to have a linear dependence on speed [15]. In this numerical evaluation, the same relation is observed. The average values of the coherence time are in harmony with available references and approximation formula for the coherence time in the literature. Regarding the fixed scatterers case in [16] it was stated that the coherence time of a UWB channel may take values up to 200 ms. In [17], the coherence time of the UWB channel is selected as 10 ms, which corresponds to human walking speed (≈ 2 meters/second) at the operating frequencies 3.1–4.8 GHz. In [18], an approximation formula was presented for the $coherence\,time \approx \frac{9c}{8|V|\omega}$ when $CCF = 0.5$. If in the case of a WB channel we choose $|V| = 30$ Km/h

and $\omega = 2\pi f$, $f = 2.5\,\text{GHz}$, the resulted coherence time is equal to $32.37\,\text{msec}$ which is very close to the results obtained using this model. Based on the same formula, the coherence time of a UWB channel when $f = 6.8\,\text{GHz}$ corresponds to a coherence time of $9.52\,\text{msec}$.

4. CONCLUSION

In this paper, an outdoor channel model for WB/UWB MIMO systems was proposed, with moving scatterers and moving receiver, based on the mathematical expression of a 2D space-time-frequency CCF. The impact of channel bandwidth, non-isotropic propagation and direction of the mobile station on the CCF was evaluated. The impact of scatterers' random displacements on the CCF of WB/UWB MIMO channels was investigated in terms of temporal, frequency, and spatial correlations. The CCF expression was used to calculate the PSD and coherence time of these two types of channels. For both WB and UWB channels, the PSD is a non-bandlimited process and reflects the channel variations caused by the mobile station speed and direction and the dispersion of the signal energy caused by the moving scatterers. To achieve uncorrelated MISO channels, it is necessary to have small coherence time values which are much easier to achieve for UWB signals with a bandwidth much larger than the coherence time of the channel. Results may be effectively employed in fields such as networking and signal processing where the channel time variations are important, e.g., signal detection, recognition, interception.

REFERENCES

1. Chelli, A. and M. Patzold, "The impact of fixed and moving scatterers on the statistics of MIMO vehicle-to-vehicle channels," *Proc. 2009 Veh. Technol. Conf.*, 1–6, 2009.
2. Molisch, A.F., "Ultrawideband propagation channels — Theory, measurement, and modeling," *IEEE Transactions on Vehicular Technology*, Vol. 54, No. 5, 1528–1545, 2005.
3. Vizitiu, I. C., *Fundamentals of Electronic Warfare*, MatrixRom Publishing House, 2011.
4. Wang, Y., X. Yu, Y. Zhang, H. Lv, T. Jiao, G. Lu, W. Z. Li, Z. Li, X. Jing, and J. Wang, "Using Wavelet entropy to distinguish between humans and dogs detected by UWB radar," *Progress In Electromagnetics Research*, Vol. 139, 335–352, 2013.
5. Zhou, W., J.-T. Wang, H. W. Chen, and X. Li, "Signal model and moving target detection based on MIMO synthetic aperture radar," *Progress In Electromagnetics Research*, Vol. 131, 311–329, 2012.
6. Waadt, E., S. Wang, C. Kocks, A. Burnic, D. Xu, G. H. Bruck, and P. Jung, "Positioning in multiband OFDM UWB utilizing received signal strength," *Proc. 7th Workshop Positioning Navigation and Communication*, 308–312, 2010.
7. Li, W. Z., Z. Li, H. Lv, G. Lu, Y. Zhang, X. Jing, S. Li, and J. Wang, "A new method for non-line-of-sight vital sign monitoring based on developed adaptive line enhancer using low centre frequency UWB radar," *Progress In Electromagnetics Research*, Vol. 133, 535–554, 2013.
8. Mizui, K., M. Uchida, and M. Nakagawa, "Vehicle-to-vehicle communication and ranging system using spread spectrum technique" *Proc. IEEE Veh. Technol. Conf.*, 335–338, May 1993.
9. Sturm, C. and W. Wiesbeck, "Waveform design and signal processing aspects for fusion of wireless communications and radar sensing," *Proceedings of the IEEE*, Vol. 99, No. 7, 1236–1259, 2011.
10. Donnet, B. J. and I. D. Longstaff, "Combining MIMO radar with OFDM communications," *Proc. 3rd European Radar Conf.*, 37–40, Sep. 2006.
11. CEPT Report 34: Report B from CEPT to European Commission in response to the Mandate 4 on Ultra-Wideband (UWB), 2009.
12. Pіştea, A. M., T. Palade, A. Moldovan, and H. Saligheh Rad, "The impact of antenna directivity and channel bandwidth on the power spectral density of wideband and UWB MISO channels," *Proc. 2011 Int. Conf. on Wireless and Mobile Comm.*, 36–41, 2011.
13. Saligheh Rad, H. and S. Gazor, "The Effect of mobile station rotation on a correlationmodel for microcellular environments" *Proc. 2004 of Global Telecomm. Conf.*, 3058–3062, 2004.

14. Papoulis, A. and U. Pillais, *Probability, Random Variables, and Stochastic Processes*, 4th edition, McGraw-Hill, 2002.

15. Jakes, W. C., *Microwave Mobile Communications*, Wiley, NY, 1974.

16. Merz, R. and J. Y. Le Boudec, "Conditional bit error rate for an impulse radio UWB channel with interfering users" *Proc. 2005 IEEE Int. Conf. on UWB*, 130–135, 2005.

17. Rangnekar, A. and K. M. Sivalingam, "Multiple channel scheduling in UWB based IEEE 802.15.3 networks," *Proc. 2004 First Int. Conf. on Broadband Networks*, 406–415, 2004.

18. Stuber, G. L., *Principles of Mobile Communicatio*n, Kluwer, Boston, MA, 1996.